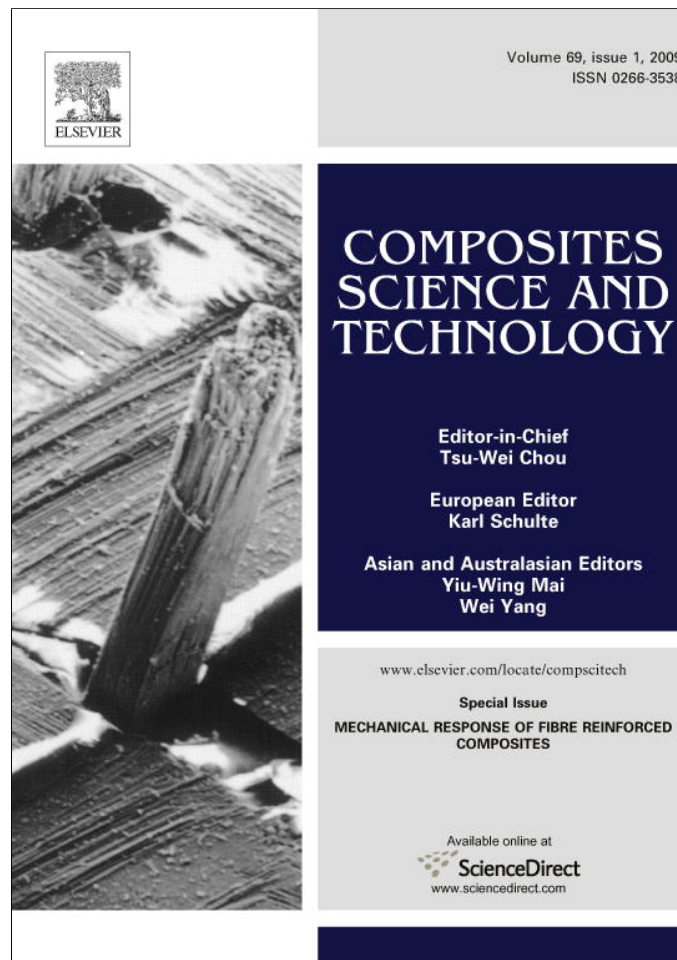


Provided for non-commercial research and education use.
Not for reproduction, distribution or commercial use.



This article appeared in a journal published by Elsevier. The attached copy is furnished to the author for internal non-commercial research and education use, including for instruction at the authors institution and sharing with colleagues.

Other uses, including reproduction and distribution, or selling or licensing copies, or posting to personal, institutional or third party websites are prohibited.

In most cases authors are permitted to post their version of the article (e.g. in Word or Tex form) to their personal website or institutional repository. Authors requiring further information regarding Elsevier's archiving and manuscript policies are encouraged to visit:

<http://www.elsevier.com/copyright>



ELSEVIER

Available online at www.sciencedirect.com

Composites Science and Technology 69 (2009) 17–21

**COMPOSITES
SCIENCE AND
TECHNOLOGY**

www.elsevier.com/locate/compscitech

Prediction of local hygroscopic stresses for composite structures – Analytical and numerical micro-mechanical approaches

F. Jacquemin ^{*}, S. Fréour, R. Guillén

*Institut de Recherche en Génie Civil et Mécanique UMR CNRS 6183, Université de Nantes – École Centrale de Nantes, 37,
Boulevard de l'Université, BP 406, 44 602 Saint-Nazaire Cedex, France*

Received 11 May 2007; accepted 11 October 2007
Available online 4 November 2007

Abstract

The aim of this article is to propose an analytical micro-mechanical self-consistent approach dedicated to mechanical states prediction in both the fiber and the matrix of composite structures submitted to a transient hygroscopic load. The time and space dependent macroscopic stresses, at ply scale, are determined by using continuum mechanics formalism. The reliability of the new approach is checked, for carbon–epoxy composites, through a comparison between the local stress states calculated in both the resin and fiber according to the new closed-form solutions and the equivalent numerical model.

© 2007 Elsevier Ltd. All rights reserved.

Keywords: A. Polymer–matrix composites; B. Hygrothermal effects; B. Microstructure; C. Residual stresses; C. Stress concentrations

1. Introduction

Moisture diffusion within an epoxy matrix based composite structure exposed to humid environmental conditions induces two types of internal stresses: the macroscopic stresses (at the scale of the composite plies) and the microscopic stresses (experienced by the elementary constituents of a considered ply). Macroscopic stresses induced by gradients of moisture concentration and/or the heterogeneity of the coefficients of moisture expansion are determined using continuum mechanics classical formalism. This method enables taking into account both space and time effects on moisture diffusion in the composite structure [1]. Localization of the macroscopic mechanical states at microscopic scale leads to different stresses in the matrix and the fiber. The discrepancies come from the strong heterogeneities of elastic properties, coefficients of moisture expansion and moisture content of the composite plies constituents. Scale transition models are often used in order to achieve the localization procedure.

In the present work, a self-consistent hygro-elastic model, based on Eshelby [2] and Kröner [3] pioneering papers, is developed in order to determine the microscopic mechanical states in a composite ply. This model takes into account the microstructure of the constituents (in particular, the reinforcing fibers morphology) and the heterogeneous microscopic moisture content (actually the reinforcing carbon fibers do not absorb moisture, which is consequently concentrated in the polymer–matrix). The classical purely numerical approach is firstly achieved, then closed-form solution for the local mechanical states are proposed in the second part of this article.

2. Hygro-elastic micro-mechanical approach

2.1. Self-consistent estimates (SC) for hygro-elastic properties

The material is investigated at two different scales for the needs of micro-mechanical modeling: the average behavior of a ply, defines the macroscopic scale, denoted by the superscript *I*, the properties and mechanical states of the matrix and fiber are respectively indicated by the

^{*} Corresponding author. Tel.: +33 2 40 17 26 25; fax: +33 2 40 17 26 18.
E-mail address: frederic.jacquemin@univ-nantes.fr (F. Jacquemin).

superscripts m and f . These constituents define the microscopic (or local) scale of the material.

The hygro-elastic behavior of the material satisfies:

$$\boldsymbol{\sigma}^\alpha = \mathbf{L}^\alpha : (\boldsymbol{\varepsilon}^\alpha - \beta^\alpha \Delta C^\alpha) \quad (1)$$

where α replaces the superscripts I, f or m . \mathbf{L} stands for the stiffness tensor, whereas β are the coefficients of moisture expansion (CME) and ΔC the moisture content.

The macroscopic stresses and strains are the volume average of the microscopic stresses and strains [4]:

$$\begin{aligned} \langle \boldsymbol{\sigma}^\alpha \rangle_{\alpha=f,m} &= \boldsymbol{\sigma}^I \\ \langle \boldsymbol{\varepsilon}^\alpha \rangle_{\alpha=f,m} &= \boldsymbol{\varepsilon}^I \end{aligned} \quad (2)$$

By using Eshelby's formalism, we obtain the following relation between macroscopic and microscopic fields:

$$\begin{aligned} \boldsymbol{\varepsilon}^I &= \langle (\mathbf{L}^\alpha + \mathbf{L}^I : \mathbf{R}^I)^{-1} : (\mathbf{L}^I + \mathbf{L}^I : \mathbf{R}^I) \rangle_{\alpha=f,m} \\ &: \boldsymbol{\varepsilon}^I + \langle (\mathbf{L}^\alpha + \mathbf{L}^I : \mathbf{R}^I)^{-1} : [\mathbf{L}^\alpha : \beta^\alpha \Delta C^\alpha - \mathbf{L}^I : \beta^I \Delta C^I] \rangle_{\alpha=f,m} \end{aligned} \quad (3)$$

where \mathbf{R}^I is the reaction tensor, defined by Eshelby [2], depending on elastic macroscopic stiffness and morphology assumed for the constituents.

Since this relation must be satisfied for any hygromechanical state, the first term of the right member of (3) must be equal to I , while the second term must be null. Thus, the self-consistent estimates for the macroscopic elastic stiffness (4) and the homogenised CME (5) are

$$\mathbf{L}^I = \langle (\mathbf{L}^\alpha + \mathbf{L}^I : \mathbf{R}^I)^{-1} : (\mathbf{L}^I + \mathbf{L}^I : \mathbf{R}^I) : \mathbf{L}^\alpha \rangle_{\alpha=f,m} \quad (4)$$

$$\begin{aligned} \beta^I &= \frac{1}{\Delta C^I} \mathbf{L}^{I^{-1}} \langle (\mathbf{L}^\alpha + \mathbf{L}^I : \mathbf{R}^I)^{-1} \rangle_{\alpha=f,m}^{-1} \\ &: \langle (\mathbf{L}^\alpha + \mathbf{L}^I : \mathbf{R}^I)^{-1} : \mathbf{L}^\alpha : \beta^\alpha \Delta C^\alpha \rangle_{\alpha=f,m} \end{aligned} \quad (5)$$

when the equilibrium state is reached, the moisture contents for the ply ΔC^I and for the neat resin ΔC^m are linked by the Eq. (6)

$$\frac{\Delta C^m}{\Delta C^I} = \frac{\rho^I}{v^m \rho^m} \quad (6)$$

where v^m stands for the volume fraction of matrix in the considered ply, ρ^I and ρ^m are respectively the composite and resin densities.

Introducing (6) in (5) and assuming that fibers do not absorb water (case of carbon/epoxy composites), the CME are then expressed [5]:

$$\beta^I = \frac{\rho^I}{\rho^m} \mathbf{L}^{I^{-1}} \langle (\mathbf{L}^\alpha + \mathbf{L}^I : \mathbf{R}^I)^{-1} \rangle_{\alpha=f,m}^{-1} : (\mathbf{L}^m + \mathbf{L}^I : \mathbf{R}^I)^{-1} : \mathbf{L}^m : \beta^m \quad (7)$$

2.2. Microscopic mechanical states

Since the carbon fiber do not absorb water, the stress-strain relation (1) rewrites

$$\boldsymbol{\sigma}^f = \mathbf{L}^f : \boldsymbol{\varepsilon}^f \quad (8)$$

In that case, Eshelby's formalism leads to the following scale transition relation for the microscopic strains experienced by the fibers:

$$\boldsymbol{\varepsilon}^f = (\mathbf{L}^f + \mathbf{L}^I : \mathbf{R}^I)^{-1} : (\boldsymbol{\sigma}^f + \mathbf{L}^I : \mathbf{R}^I : \boldsymbol{\varepsilon}^I) \quad (9)$$

Eq. (9) enables to determine the microscopic strains in the fiber from the macroscopic stresses and strains. Thereafter, Eq. (8) is used in order to find the fiber stresses. The microscopic mechanical states experienced by the matrix are thereafter deduced from Hill volume averages (2):

$$\begin{cases} \boldsymbol{\sigma}^m = \frac{1}{v^m} \boldsymbol{\sigma}^I - \frac{v^f}{v^m} \boldsymbol{\sigma}^f \\ \boldsymbol{\varepsilon}^m = \frac{1}{v^m} \boldsymbol{\varepsilon}^I - \frac{v^f}{v^m} \boldsymbol{\varepsilon}^f \end{cases} \quad (10)$$

3. Towards an analytical self-consistent model

3.1. Closed-form solution of Morris' tensor

The self-consistent framework is based on the mechanical treatment of the interactions between ellipsoidal heterogeneous inclusions (microscopic scale) and the embedding homogeneous equivalent medium (macroscopic scale). The average macroscopic elastic properties \mathbf{L}^I of the composite are related to the morphology assumed for elementary inclusions, through Morris' tensor \mathbf{E}^I . Actually, the reaction tensor \mathbf{R}^I introduced in Eq. (3) writes

$$\mathbf{R}^I = (\mathbf{L}^{I^{-1}} - \mathbf{E}^I) : \mathbf{E}^{I^{-1}} \quad (11)$$

Originally, spherical inclusions only were considered by Morris [6]. For ellipsoidal shaped inclusions Asaro and Barnett [7] and Kocks et al. [8] have established the following relations for numerical calculation of each $ijkl$ subscripted component of Morris' tensor

$$\begin{cases} \mathbf{E}_{ijkl}^I = \frac{1}{4\pi} \int_0^\pi \sin \theta d\theta \int_0^{2\pi} \gamma_{ijkl} d\phi \\ \gamma_{ijkl} = K_{ik}^{-1}(\xi) \xi_j \xi_l \end{cases} \quad (12)$$

Some analytical forms for Morris' tensor are available in the literature: Mura [9], Kocks et al. [8] and Qiu and Weng [10] for example. Nevertheless, these forms were established considering either spherical, disc-shaped or fiber-shaped inclusions embedded in an ideally isotropic macroscopic medium, that is incompatible with the strong elastic anisotropy exhibited by fiber-reinforced composites at macroscopic scale. In the case of fiber-reinforced composites, a transversely isotropic macroscopic elastic behavior being coherent with fiber shape is actually expected (and predicted by the numerical computations). This is compatible with the following form of \mathbf{K} tensor

$$\mathbf{K} = \begin{bmatrix} L_{55}^I(\xi_2^2 + \xi_3^2) & (L_{12}^I + L_{55}^I)\xi_1\xi_2 & (L_{12}^I + L_{55}^I)\xi_1\xi_3 \\ (L_{12}^I + L_{55}^I)\xi_1\xi_2 & L_{22}^I\xi_2^2 + L_{44}^I\xi_3^2 & (L_{23}^I + L_{44}^I)\xi_2\xi_3 \\ (L_{12}^I + L_{55}^I)\xi_1\xi_3 & (L_{23}^I + L_{44}^I)\xi_2\xi_3 & L_{44}^I\xi_2^2 + L_{22}^I\xi_3^2 \end{bmatrix} \quad (13)$$

where $\xi_1 = \frac{\sin \theta \cos \phi}{a_1}$, $\xi_2 = \frac{\sin \theta \sin \phi}{a_2}$ and $\xi_3 = \frac{\cos \theta}{a_3}$. Assuming that the longitudinal (subscripted₁) axis is parallel to fiber

axis, one obtains the following conditions for the semi-lengths of the microstructure representative ellipsoid: $a_1 \rightarrow \infty$, $a_2 = a_3$.

The determination of Morris' tensor requires the determination of the inverse of \mathbf{K} tensor. Due to the above listed conditions over the dimensions a_1 , a_2 and a_3 of the considered fiber-shaped inclusions, drastic simplifications of Morris' tensor occur:

$$\mathbf{E}^J = \begin{bmatrix} 0 & 0 & 0 & 0 & 0 & 0 \\ 0 & \frac{3}{8L_{22}^J} + \frac{1}{4L_{22}^J - 4L_{23}^J} & \frac{L_{22}^J + L_{23}^J}{8L_{22}^J L_{23}^J - 8L_{22}^J{}^2} & 0 & 0 & 0 \\ 0 & \frac{L_{22}^J + L_{23}^J}{8L_{22}^J L_{23}^J - 8L_{22}^J{}^2} & \frac{3}{8L_{22}^J} + \frac{1}{4L_{22}^J - 4L_{23}^J} & 0 & 0 & 0 \\ 0 & 0 & 0 & \frac{1}{8L_{22}^J} + \frac{1}{4L_{22}^J - 4L_{23}^J} & 0 & 0 \\ 0 & 0 & 0 & 0 & \frac{1}{8L_{55}^J} & 0 \\ 0 & 0 & 0 & 0 & 0 & \frac{1}{8L_{55}^J} \end{bmatrix} \quad (14)$$

3.2. Analytical solutions for the microscopic stresses

The epoxy matrix is usually isotropic, so that three components only have to be considered for its elastic constants: L_{11}^m , L_{12}^m and $L_{44}^m = \frac{L_{11}^m - L_{12}^m}{2}$. One moisture expansion coefficient is sufficient to describe the hygroscopic behavior of the matrix: β_{11}^m .

In the case of the carbon fibers, a transverse isotropy is generally observed. Thus, the corresponding elasticity constants depend on the following components: L_{11}^f , L_{12}^f , L_{22}^f , L_{23}^f , L_{44}^f , and L_{55}^f . Moreover, since the carbon fiber does not absorb water, its CME β_{11}^f and β_{22}^f will not be involved in the mechanical states determination. Introducing these additional assumptions in Eq. (3), and taking into account the form (14) obtained for Morris' tensor, the following general expressions are found for the components of the strain tensor experienced by the matrix

$$\begin{cases} \epsilon_{11}^m = \epsilon_{11}^J \\ \epsilon_{12}^m = \frac{2L_{55}^J \epsilon_{12}^J}{L_{55}^J + L_{44}^m} \\ \epsilon_{13}^m = \frac{2L_{55}^J \epsilon_{13}^J}{L_{55}^J + L_{44}^m} \\ \epsilon_{22}^m = \frac{N_1^m + N_2^m + N_3^m + N_4^m}{D_1^m} \\ \epsilon_{23}^m = \frac{2L_{22}^J (L_{22}^J - L_{23}^J) \epsilon_{23}^J}{2L_{22}^J{}^2 + L_{23}^J (L_{44}^m - L_{44}^m) + L_{22}^J (3L_{44}^m - 2L_{23}^J - 3L_{44}^m)} \\ \epsilon_{33}^m = \epsilon_{22}^m - 4L_{22}^J \frac{(L_{22}^J - L_{23}^J) (\epsilon_{22}^J - \epsilon_{33}^J)}{L_{22}^J{}^2 + 3L_{22}^J (L_{11}^m - L_{12}^m) - L_{23}^J (L_{11}^m + L_{23}^J - L_{12}^m)} \end{cases} \quad (15)$$

$$\text{where } \begin{cases} N_1^m = \beta_{11}^m (L_{11}^m + 2L_{12}^m) \Delta C^m \\ \quad - (\beta_{11}^J L_{12}^J + \beta_{22}^J (L_{22}^J + L_{23}^J)) \Delta C^J \\ N_2^m = (L_{12}^J - L_{12}^m) \epsilon_{11}^J \\ N_3^m = \frac{L_{22}^J \{ L_{22}^J (5L_{11}^m - L_{12}^m + 3L_{22}^J) - L_{23}^J (3L_{11}^m + L_{12}^m + 4L_{22}^J) + L_{23}^J{}^2 \}}{(3L_{22}^J - L_{23}^J) (L_{11}^m - L_{12}^m) + L_{22}^J{}^2 - L_{23}^J{}^2} \epsilon_{22}^J \\ N_4^m = \frac{L_{22}^J \{ L_{22}^J (L_{11}^m - 5L_{12}^m - L_{22}^J) + L_{23}^J (L_{11}^m + 3L_{12}^m + 4L_{22}^J) - 3L_{23}^J{}^2 \}}{(3L_{22}^J - L_{23}^J) (L_{11}^m - L_{12}^m) + L_{22}^J{}^2 - L_{23}^J{}^2} \epsilon_{33}^J \\ D_1^m = L_{11}^m + L_{12}^m + L_{22}^J - L_{23}^J \end{cases}$$

The corresponding analytical form for the microscopic stress tensor in the matrix comes from (1):

$$\sigma^m = \begin{bmatrix} \sigma_{11}^m & 2L_{44}^m \epsilon_{12}^m & 2L_{44}^m \epsilon_{13}^m \\ 2L_{44}^m \epsilon_{12}^m & \sigma_{22}^m & 2L_{44}^m \epsilon_{23}^m \\ 2L_{44}^m \epsilon_{13}^m & 2L_{44}^m \epsilon_{23}^m & \sigma_{33}^m \end{bmatrix} \quad (16)$$

$$\text{with, } \begin{cases} \sigma_{11}^m = L_{11}^m \epsilon_{11}^m + L_{12}^m (\epsilon_{22}^m + \epsilon_{33}^m) - \beta_{11}^m (L_{11}^m + 2L_{12}^m) \Delta C^m \\ \sigma_{22}^m = L_{11}^m \epsilon_{22}^m + L_{12}^m (\epsilon_{11}^m + \epsilon_{33}^m) - \beta_{11}^m (L_{11}^m + 2L_{12}^m) \Delta C^m \\ \sigma_{33}^m = L_{11}^m \epsilon_{33}^m + L_{12}^m (\epsilon_{11}^m + \epsilon_{22}^m) - \beta_{11}^m (L_{11}^m + 2L_{12}^m) \Delta C^m \end{cases}$$

The local mechanical states in the fiber are provided by Hill's average laws (2).

4. Example

Thin laminated composite pipes, with thickness 4 mm, initially dry then exposed to an ambient fluid, made up of T300/5208 carbon–epoxy plies are considered for the determination of both macroscopic stresses and moisture content as a function of time and space. Table 1 presents the elastic properties considered for the T300 carbon fiber, N5208 epoxy matrix and the effective stiffness deduced from the self-consistent approach for a fiber volume fraction of 60% in the composite ply. The coefficients of moisture expansion obtained through the same approach are: $\beta_{11}^f = 0.035$ and $\beta_{22}^f = 1.026(\beta_{11}^m = 0.6)$.

Fig. 1 shows the time-dependent concentration profiles, satisfying an unidirectional Fick's law, resulting from the application of a boundary concentration $c_0 = 1.5\%$, as a function of the normalized radial distance from the inner radius r_{dim} . At the beginning of the diffusion process important concentration gradients occur near the external surfaces. The permanent concentration (noticed *perm* in the caption) holds with a constant value because of the symmetrical hygroscopic loading.

Starting with the macroscopic stresses deduced from continuum mechanics (CM), the local stresses in both the fiber and matrix were calculated either with the new analytical forms or the fully numerical model. The comparison between the two approaches is plotted on Fig. 2 which

Table 1
Mechanical properties

	E_1 (GPa)	E_2, E_3 (GPa)	ν_{12}, ν_{13}	G_{23} (GPa)	G_{12} (GPa)
Fiber T300	230	15	0.2	7	15
Epoxy matrix N 5208	4.5	4.5	0.4	1.6	1.6
T300/5208	139.6	9.8	0.28	3.5	6.4

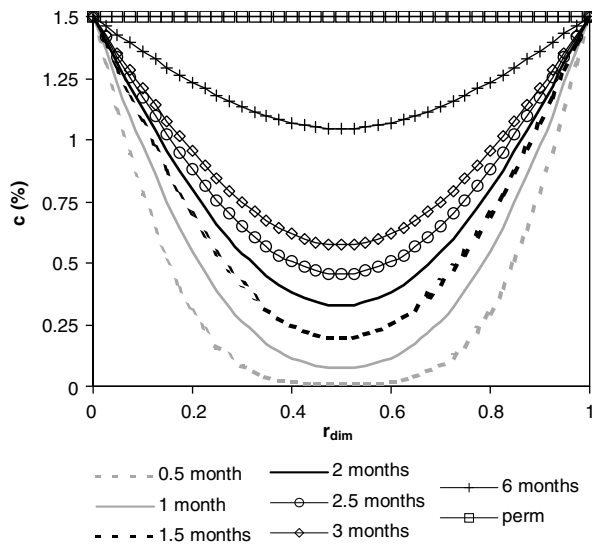


Fig. 1. Moisture concentration.

shows the obtained results for the transverse (σ_{22}) and shear (σ_{12}) stresses for the central ply of a unidirectional composite and in the case of a $[55/-55]_S$ laminate (for the UD composite the shear stress is null at any scale). The Fig. 2 demonstrates the very good agreement between the numerical approach and the corresponding closed-form solutions whatever the stress component and the stacking sequence. The slight differences appearing are due to the small deviations on the components of Morris' tensor calculated using the two approaches.

Actually, it is not possible to assume the quasi-infinite length of the fiber along the longitudinal axis in the case of the numerical approach, because the numerical computation of Morris' tensor is highly time-consuming. Thus, the numerical SC model constitutes only an approximation of the real microstructure of the composite. In consequence, it seems that the new analytical forms, that are able to take into account the proper microstructure for the fibers, are not only more convenient, but also more reliable than the initially proposed numerical approach.

The highest level of macroscopic tensile stress is reached for the unidirectional (UD) composite, in the transverse direction and in the central ply of the structure (50 MPa, cf. Fig. 2). The transverse stresses probably exceed the macroscopic tensile strength in this direction. The choice of a $[+55^\circ/-55^\circ]_S$ laminated allows to reduce the macroscopic stress in the transverse direction where the upper level falls down to 25 MPa. Nevertheless, a high shear stress rises along the time in the fibers of the central ply of such a structure (35 MPa), and the matrix experiences strong compressive stresses that can reach -185 MPa in the studied example.

Others calculations show that important stresses occur in surface where the epoxy matrix is submitted to high compressive stresses: $\sigma_{11} = -280$ MPa, $\sigma_{22} = -225$ MPa, $\sigma_{33} = -140$ MPa. These local stresses could help to explain damage occurrence in the surface of composite structures submitted to such hygroscopic conditions.

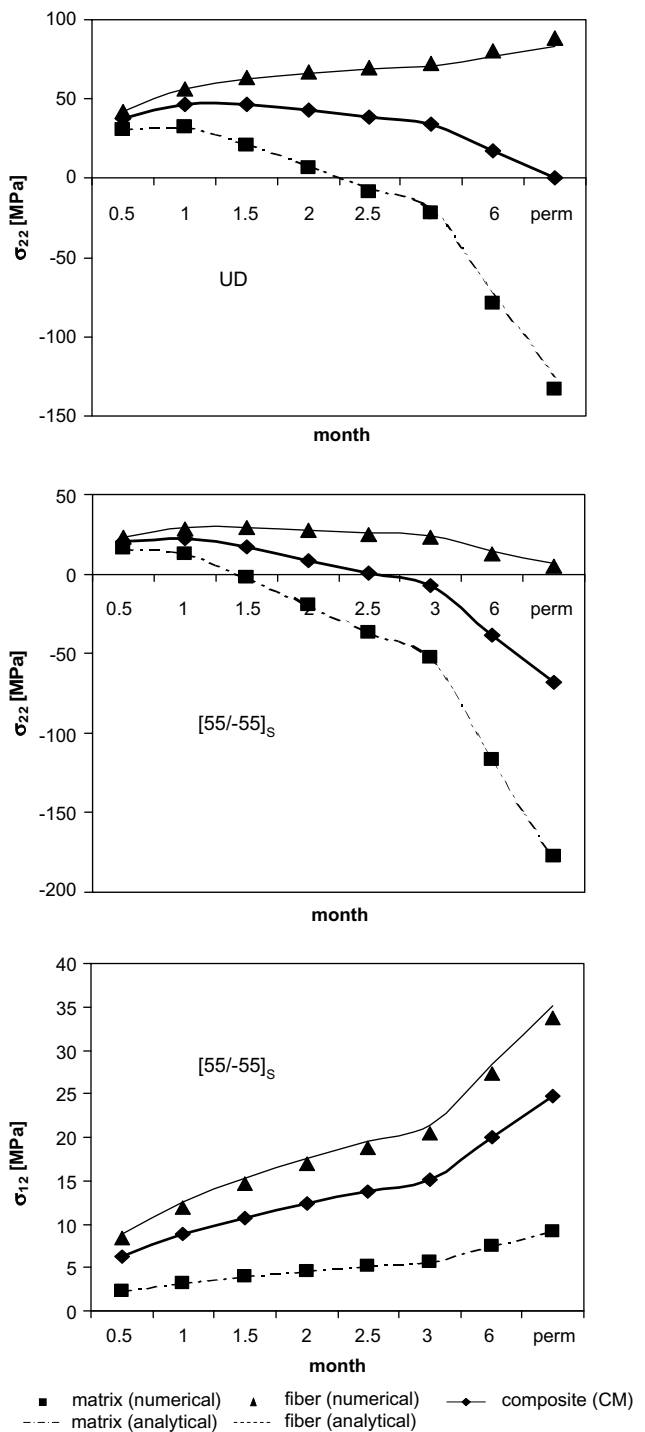


Fig. 2. Analytical and numerical predictions of hydro-elastic stresses.

5. conclusion

In the present paper, an analytical self-consistent model, for the calculation of local hydro-elastic strains and stresses, is proposed. The first step of this approach is to analytically express Morris' tensor. The new closed-form solutions obtained for the components of Morris' tensor were introduced in the classical hydro-elastic scale transition relation in order to find closed-form solutions for the local internal

strains and stresses. The closed-form solutions demonstrated in the present work were compared to the fully numerical hygro-elastic self-consistent model for various stacking sequences: unidirectional or laminated composites. A very good agreement is obtained between the two models for any component of the local stress tensors. The present analytical model, that works faster and is more convenient to program than the classical model, could be implemented in a calculation code combining both the continuum mechanics formalisms (necessary to determine the macroscopic stresses and strains in each ply) and the micro-mechanical model. This new software will constitute an accurate and powerful tool for the prediction of a possible damage in the material at every scale of a composite structure submitted to a transient hygroscopic stress.

References

- [1] Jacquemin F, Vautrin A. A closed-form solution for the internal stresses in thick composite cylinders induced by cyclical environmental conditions. *Compos Struct* 2002;58:1–9.
- [2] Eshelby JD. The determination of the elastic field of an ellipsoidal inclusion, and related problems. *Proc R Soc London A* 1957;241:376–96.
- [3] Kröner E. Berechnung der elastischen Konstanten des Vielkristalls aus den Konstanten des Einkristalls. *Z Phys* 1958;151:504–18.
- [4] Hill R. The essential structure of constitutive laws for metals composites and polycrystals. *J Mech Phys Solids* 1967;15:79–95.
- [5] Jacquemin F, Fréour S, Guillén R. A hygro-elastic self-consistent model for fiber-reinforced composites. *J Reinf Plast Compos* 2005;24:485–502.
- [6] Morris PR. Elastic constants of polycrystals. *Int J Eng Sci* 1970;8:49–61.
- [7] Asaro RJ, Barnett DM. The non-uniform transformation strain problem for an anisotropic ellipsoidal inclusion. *J Mech Phys Solids* 1975;23:77–83.
- [8] Kocks UF, Tomé CN, Wenk HR. *Texture and anisotropy*. Cambridge University Press; 1988.
- [9] Mura T. *Micromechanics of defects in solids*. The Hague, Netherlands: Martinus Nijhoff Publishers; 1982.
- [10] Qiu YP, Weng GJ. The influence of inclusion shape on the overall elastoplastic behavior of a two-phase isotropic composite. *Int J Solids Struct* 1991;27:1537–50.